RAILWAY FORMATION DESIGN INCORPORATING THE BENEFITS OF MECHANICAL STABILISATION OF SUB-BALLAST

K. Zamara, A. Lees

Tensar International Ltd
Blackburn, UK

KEYWORDS: trackbed design, geogrid, finite element modelling

ABSTRACT

A design method for conventional railway track formations with mechanically stabilised sub-ballast layers to limit deformations in fine-grained subgrades is proposed. It is based on previous performance-based design methods with the important distinction that two-dimensional mechanisms are considered. An advanced non-linear strength constitutive model for the mechanically stabilised sub-ballast and a hardening plasticity model for the subgrade are used to predict permanent deformation under a single loading directly, rather than by elastic analysis and approximate empirical transfer functions. Empirical relationships are then used to predict permanent deformation accumulation of the subgrade under successive loadings. A small parametric study using this approach identified a significant improvement in terms of subgrade stress and track bearing capacity with mechanical stabilisation of the sub-ballast layer. The same performance as non-stabilised sub-ballast could be achieved with thinner layers of mechanically stabilised sub-ballast, bringing savings in time, cost and carbon footprint.

NOTATION

b	Empirical subgrade characterisation value
h	Ballast and sub-ballast combined thickness
k	Spring stiffness
q	Deviatoric stress
s_u	Undrained shear strength of clay subgrade
A	Permanent or plastic strain in subgrade following single loading
A_ρ	Permanent or plastic vertical displacement of subgrade following single loading
B	Sleeper width
C	Inter-bogie axle spacing between coupled bogies
D	Intra-bogie axle spacing
E	Young's modulus
G	Axle spacing between bogies of one rail vehicle
I	Second moment of area

L Sleeper length

N Number of design wheel load repetitions

P Wheel load

P_f Wheel load at track bearing capacity

ε_1 Major principal strain

$\varepsilon_{1,p}$ Major principal plastic strain

ε_p Plastic or permanent strain

ν Poisson's ratio

ρ_p Permanent or plastic subgrade vertical displacement

φ' Internal friction angle

ψ Dilatancy angle

INTRODUCTION

This paper describes an approach to the design of rail formations constructed on fine-grained subgrades that can take account of the mechanical stabilisation by geogrid of the sub-ballast layer. The design objective is to limit plastic deformations of the subgrade to prevent reconstruction of the formation during the design life of the railway. Deformations within the ballast layer can be managed through maintenance while the sub-ballast is usually composed of a well-graded and highly compacted granular layer and relatively small deformations occur. The majority of permanent deformation below ballast occurs in the fine-grained subgrade layers and could require costly reconstruction of the formation. Deformations in a fine-grained layer are caused by several mechanisms (Li et al, 2016). The mechanism addressed here is progressive shear failure resulting in a permanent subgrade strain and deformation. In extreme cases, the subgrade can eventually heave through the ballast layers as shown in Figure 1.

Design options to control deformations include adjusting the granular layer thickness. The Li and Selig (1998a,b) method for predicting the accumulation of permanent subgrade strain ε_p for N repetitions of a load adopts the commonly used Equation 1 for fine-grained soils. The Li and Selig (1998a,b) method is widely used and has been adopted by Burrow et al (2017) and Sayeed and Shahin (2018a,b). The A parameter is the permanent strain following the first axle load. The accumulation of permanent strain with N repetitions of the axle load is defined by the b parameter.

Equation 1 can be viewed as a semi-empirical approach that relates vertical surface settlement to progressive shear failure in the subgrade through the parameter A. Li and Selig (1998a) acknowledged that there was uncertainty in the prediction of ε_p on the first load (i.e. the A parameter) using their proposed empirical relationship and deviatoric stress q determined by elastic layer analysis.

The *b* parameter is relatively straightforward to determine and depends only on the subgrade soil type as shown in Table 1. Li et al (2016) state that parameter *b* is reasonably invariant to deviator stress and soil physical state and can be considered constant for a soil material type.

Fig. 1 Example of progressive shear failure of subgrade at Victoria, Texas

$$\epsilon_p = AN^b \qquad \text{(Eqn. 1)}$$

Table. 1. Li and Selig (1998a) subgrade soil types.

Soil type	*b*
CH (plastic clay)	0.18
CL (non-plastic clay)	0.16
MH (plastic silt)	0.13
ML (non-plastic silt)	0.10

Three-dimensional (3D) FEM can be used to assess stress and strain profiles in the formation including multiple axles. Sayed and Shahin (2018) and Burrow et al (2017) used 3D FEM to assess stress and strain profiles in the ground under a single multi-axle load and then used 1D calculations for deformation. One limitation of this approach is duplication of effort. First 3D FEM is used to generate stresses and strains in the ground then the *A* factor is assessed then 1D integration of effects is performed. Similarly, if the effects of geogrid on formation performance is to be assessed again a 3D FEM would be used to generate a distribution of stress and strain followed by a 1D calculation.

Lees and Kelly (2023) overcame these shortcomings by using 3D FEM with advanced hardening plasticity constitutive models for the subgrade to predict permanent deformation under a single loading (the *A* parameter) directly, rather than by elastic analysis and approximate empirical transfer functions. Permanent deformations from single loadings are then multiplied by the simple empirical relationship in Equation 2 to include their accumulation from load repetitions. They undertook a sensitivity analysis and parametric study using the validated 3D FEM model to derive simple, approximate equations to determine permanent subgrade strain and deformation that could be used for routine design without the need for a full design by FEM.

$$\rho_p = A_\rho N^b \qquad \text{(Eqn. 2)}$$

This paper extends the same 3D FEM approach to incorporate the benefit of mechanical stabilisation of the sub-ballast layer on subgrade permanent deformation.

MECHANICALLY STABILISED LAYER

Stiff, coextruded, punched and drawn, multi-axial and multi-aperture shape geogrid incorporates features all designed primarily to restrict the movement of soil particles in and around its apertures – a function defined as stabilisation (ISO, 2018) – and there is evidence (e.g. Bussert and Cavanaugh (2010)) that the stabilising effect of geogrid extends a significant distance from the geogrid plane, typically 30 cm or more.

Lees and Clausen (2020) performed large triaxial compression tests (specimen size 0.5 m dia. x 1.0 m height) with vacuum-applied confining stress on crushed rock specimens with and without a stabilising geogrid placed at mid-height. A similar procedure was undertaken for this study on specimens of a crushed limestone aggregate of the grading shown in Figure 2. It was compacted in a split mould using a vibrating plate on 200 mm thick layers to at least 95% maximum dry density. Specimens were contained in a 4 mm thick silicone rubber membrane for which a membrane correction was applied to the confining stress to obtain σ_3. Cases with geogrid had a single layer of stiff, coextruded, punched and drawn, multi-axial and multi-aperture shape geogrid placed at the mid-height of the specimen within the third compacted layer. The composite material of this specific combination of aggregate and geogrid is referred to as *Stabilised Sub-Ballast 1* (SSB1).

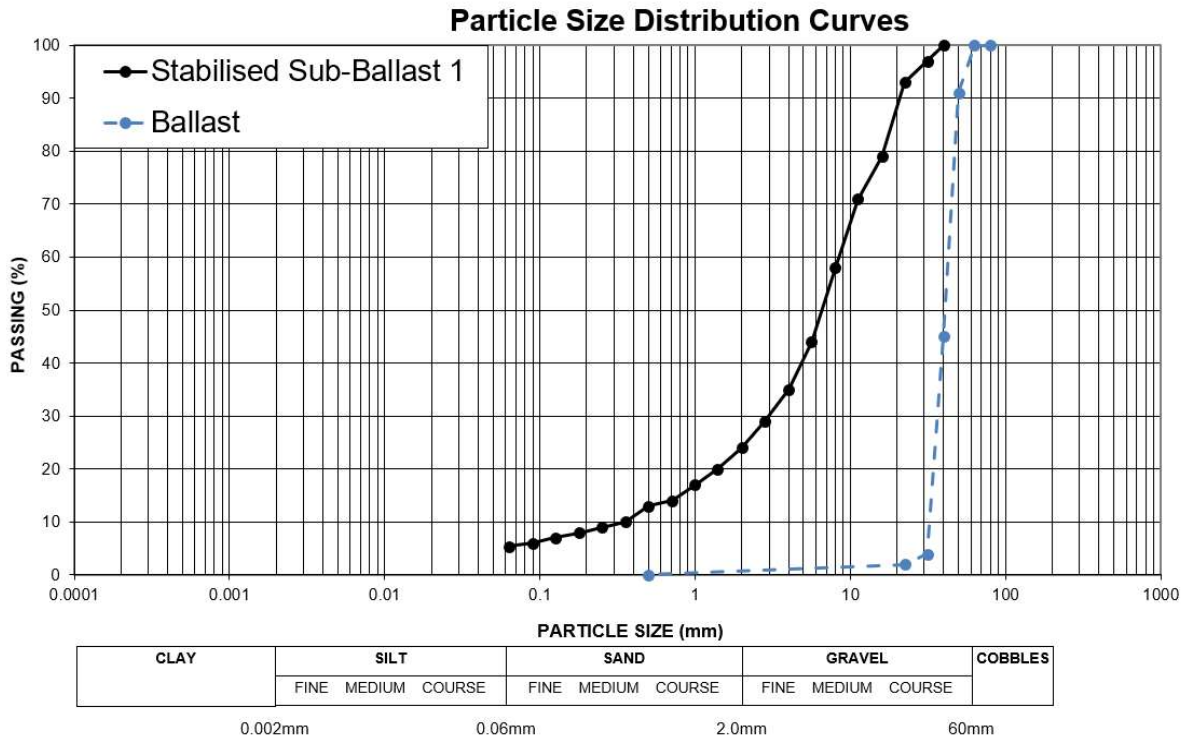

Fig 2 Particle size distribution for the aggregates used in the triaxial and ballast box studies

The plots of averaged deviatoric stress q against averaged deviatoric strain ε_q at three different confining stresses with and without the geogrid in Figure 3 show an enhanced peak shear strength in the geogrid-stabilised soil at all three confining stresses. In the legend, "N" and "S" denote non-stabilised and stabilised specimens respectively while the number shows the nominal confining stress in kPa.

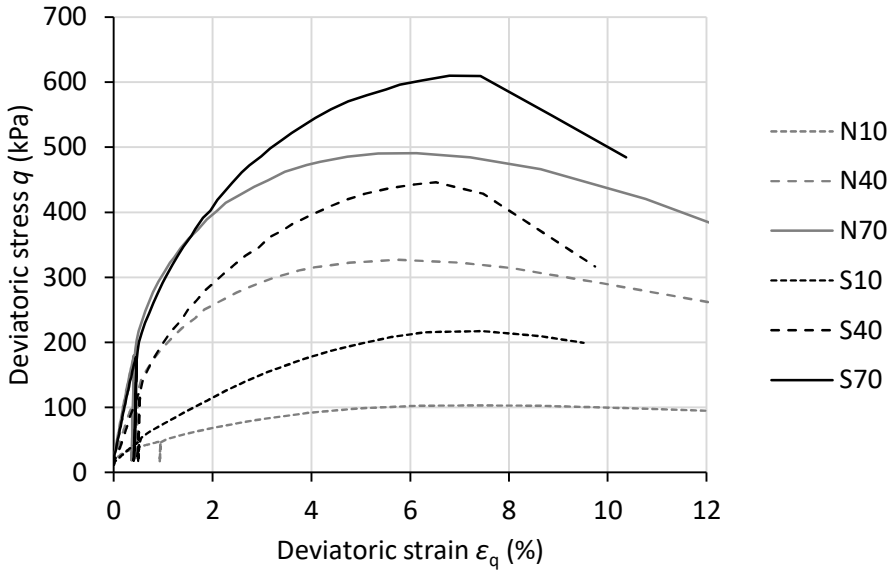

Fig. 3 q v. ε_a plots from triaxial compression tests on stabilised and non-stabilised crushed rock aggregate (sub-ballast)

A linear elastic perfectly-plastic (LEPP) constitutive model called the Tensar Stabilised Soil Model (TSSM) with the non-linear failure envelope was implemented into the Plaxis 2D Version 20 (Brinkgreve et al, 2019) FEA software and found to provide accurate predictions of failure stress in back-analyses of the triaxial compression tests (Lees and Clausen, 2020).

The TSSM strength parameters shown in Table 2 were derived by back-analysis of the triaxial tests to match the peak failure stresses reached in Figure 3. The stiffness values were selected to be appropriate for the sub-ballast but did not influence the output of subgrade permanent strain significantly, as noted by Lees and Kelly (2023).

Table. 2. TSSM input parameters for sub-ballast.

Input parameters	Sub-ballast
k_0, m_o	6.0
c_0 (kPa)	111
a_0, b_0	4.9
c_t (kPa)	400
a_t	80
γ (kN/m^3)	20
E (MPa)	100
v	0.2

PARAMETRIC STUDY

Lees and Kelly (2023) developed a static, elasto-plastic, 3D FEA model of a railway track and its foundation, validated by the full-scale trials described by Li and Selig (1998a). The same model was adapted in this study for a small parametric study incorporating mechanical stabilisation of the sub-ballast layer using the modelling approach described in the previous section. The output of this parametric study would provide an indication of the performance benefits of mechanically stabilised sub-ballast in terms of subgrade permanent strain and deformation.

FEM geometry

The parametric study was performed using Plaxis 3D Version 22 and the mesh of second order 10-noded tetrahedral elements shown in Figure 4. Three vertical planes of symmetry formed vertical boundaries to significantly reduce model size: one along the track centreline and the other two as illustrated in Figure 5. Only the distant vertical boundary parallel to the track needed to be placed sufficiently far (10 m) away from the track such that boundary effects were not significant. Similarly, the bottom boundary was placed 10 m below track level. The vertical boundaries were fixed against displacement in their normal directions and the bottom boundary fixed in all three axis directions. The relatively small model domain was sufficient for the low train speeds intended for this design approach. Higher speeds may require a larger domain to take account of dynamic effects (Connolly et al, 2020).

The ballast layer below sleeper was 0.25 m thick and the sub-ballast thickness was varied. The self-weight of the ballast above base of sleeper (assumed flush with top of sleeper) was considered as a surcharge equivalent to the top of ballast extending to a 0.15 m wide shoulder beyond end of sleeper and sloping at 1(V):2(H) down to subgrade level.

Concrete sleepers were modelled as volume elements in full contact with the underlying ballast layer without interface elements. They were 0.273 m wide, 0.205 m deep with a half-length of 1.295 m and were placed at 0.6 m centres. The rail was modelled with linear elastic beam elements positioned at 1.506 m centres (equivalent to 1.435 m gauge), connected through fasteners as spring elements to the top surface of the sleepers.

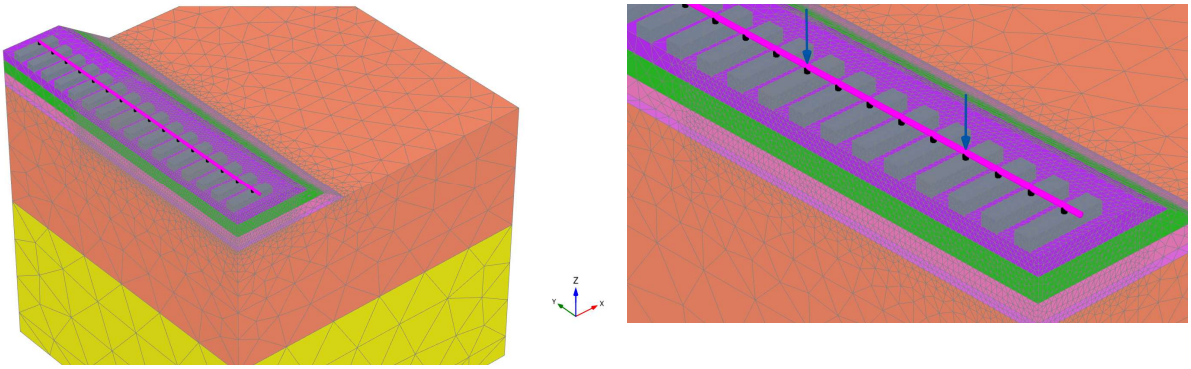

a) Whole mesh b) Close-up of loaded area

Fig. 4 FEM mesh used in parametric study

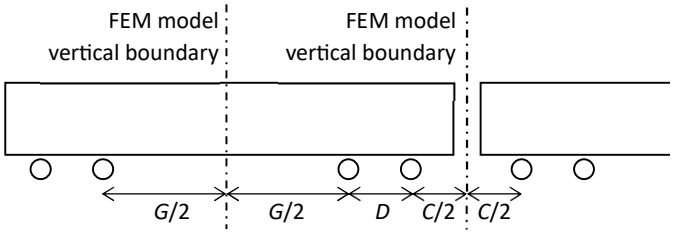

Fig. 5 Axle spacing terms and FEM model vertical boundary locations

The clay subgrade was assumed to be 4 m thick, below which was placed a dense sand layer to act as a buffer between the clay and the fixed bottom boundary to the mesh. The sand layer had an insignificant effect on the key outputs but was modelled using the Hardening Soil model (Shanz et al, 1999) with typical input parameters for a silty sand as shown in Table 3.

Table 3. Silty sand FEM input parameters.

Parameter	Value
E_{50}, E_{oed}, E_{ur} (MPa), m	20, 18, 60, 0.5

c' (kPa), φ', ψ	0.1, 30°, 0°
γ (kN/m^3), p_p (kPa), K_0	18, 60, 1.0
v_{ur}, p_{ref} (kPa),	0.2, 100
K_0^{nc}, R_f	0.5, 0.9

FEM constitutive models and input parameters

The accurate prediction of permanent subgrade strain and deformation under relatively low stress changes due to a single load application requires an advanced, hardening plasticity constitutive model. Many of those implemented into FEM programs are formulated in terms of effective stress which makes them difficult to use for fine-grained subgrades that tend to be partially saturated and often heavily over-consolidated near the surface due to desiccation, creating complex effective stress states. Consequently, the NGI-ADP hardening plasticity model formulated in terms total stresses was selected to model the clayey silt subgrade. As described by Grimstad et al (2012), anisotropic undrained shear strength s_u in three stress states active, direct shear and passive (ADP) are direct input parameters, as are the shear strains at failure in the same three states to specify the primary loading stress-strain behaviour. Although there are a large number of input parameters requiring advanced parameter testing of the type that may not be feasible on some rail projects, there are a number of published correlations, e.g. Karlsrud et al (2005), between characterisation test results and the model parameters allowing typical values to be estimated from simple tests such as that of plasticity index.

On modelling a weathered clay crust, Khan (1993) recommended K_0 values higher than 1 at the ground surface, decreasing with depth to values appropriate for the underlying clay. A similar approach was taken by D'Ignazio et al (2017) in the modelling of a partially saturated clay crust layer in the simulation of railway embankments. Since partially saturated, subgrade surface conditions were recreated in the laboratory test, a K_0 of 1.0 on total stress was adopted in the back-analyses. The input parameters adopted for the subgrade are shown in Table 4.

Table 4. NGI-ADP model input parameters for subgrade

Input parameters	Subgrade layer
γ (kN/m^3), K_0, τ_0/s_u^A	18, 1.0, 0
G_{UR}/s_u^A, ν	75, 0.495
s_u^A (kPa)	50
$s_u^{C,TX}/s_u^A$, s_u^P/s_u^A, s_u^{DSS}/s_u^A	0.99, 0.5, 0.7
γ_f^C, γ_f^E, γ_f^{DSS} (%)	18, 20, 20

The ballast was modelled using the Mohr-Coulomb model with the input parameters shown in Table 5 and the sub-ballast (with and without mechanical stabilisation) with the TSSM and the input parameters shown in Table 2. Although these linear elastic perfectly plastic (LEPP) models are simpler in terms of permanent deformation prediction, the main aim of the ballast

and sub-ballast models were to predict the distribution of applied stress through these layer to the subgrade rather than to predict permanent strain within. A similar approach was adopted by Lees and Kelly (2023) and was shown to be valid in a sensitivity analysis.

Table 5. LEPP MC model input parameters for ballast

Parameter	Value
γ (kN/m^3), K_0	19, -
φ' (deg.), c' (kPa), ψ (deg.)	45, 0.1, 15
E (MPa), ν	100, 0.2

The concrete of the half-sleeper, steel rail and fasteners were all modelled as linear elastic materials with the input parameters shown in Table 6.

Table 6. Linear elastic material model input parameters for track components

Concrete sleeper	Rail (beam)	Fastener (spring)
E = 30 GPa	E = 207 GPa	k = 100 kN/mm
ν = 0.2	A = 8.6x10^{-3} m^2	
γ = 24 kN/m^3	I = 0.03x10^{-3} m^4	
	γ = 77 kN/m^3	

Two static point loads were applied to the rail representing the wheel load with magnitude as shown in Table 7 and spacings of C=2.4, D=1.8, G=9.0 (Figure 5).

Table 7. FEM parametric study input values

Parameter	Values
Wheel load P (kN)	125, 200, 275
Sub-ballast thickness (m)	0.3, 0.6, 0.9
Geogrid	Yes, No

The analysis phases began by establishing initial stresses with the ground surface at subgrade level, zero pore water pressure and K_0 as shown in Tables 3 and 4. In successive phases the ballast layers and track elements were activated, then the wheel loads imposed and the wheel loads released to obtain the permanent deformation in the subgrade (having been reset to zero datum displacement following placement of ballast layers and track).

All combinations of wheel load and sub-ballast thickness shown in Table 7 were analysed and outputs of maximum q at the subgrade surface recorded. The ballast layer was 0.25 m thick throughout with the sub-ballast layer thickness varied. The subgrade failure strain parameters were constant and as shown in Table 4.

The output of maximum deviatoric stress q_{max} at the subgrade surface in all the cases is plotted in Figure 6 and compared between cases with and without mechanical stabilisation of the sub-ballast with all other input parameters equal. It provides an indication of the load

spreading and subgrade stress reduction effect of the mechanical stabilisation of the sub-ballast. This, in turn, results in lower permanent subgrade strain ε_p. In other words, thinner mechanically stabilised sub-ballast layers may be installed to achieve the same performance as thicker non-stabilised sub-ballast layers in terms of ε_p. This would bring economies in construction in terms of cost, time and carbon footprint.

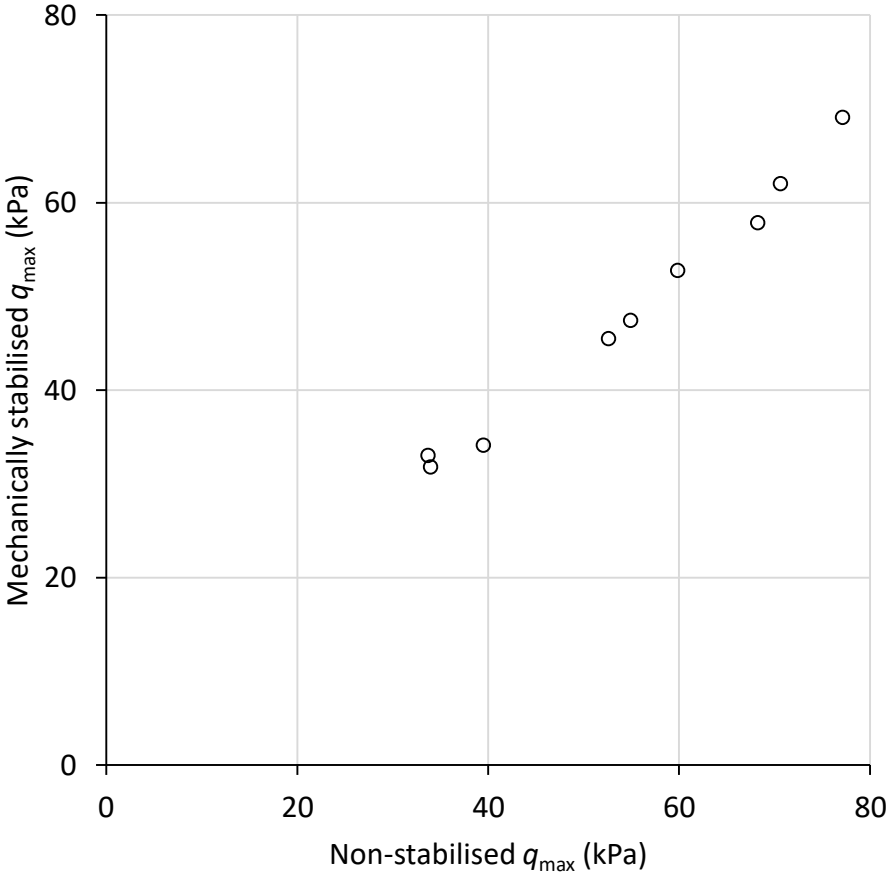

Fig. 6 Output of maximum q at subgrade surface compared between non-stabilised and mechanically stabilised sub-ballast.

A further parametric study was undertaken by replacing the point loads with imposed vertical, downwards displacement of 0.5 m at the same locations. All three values of sub-ballast thickness shown in Table 7 were run. The purpose of this part of the parametric study was to determine the track bearing capacity, which was taken as the total vertical load at 0.5 m vertical displacement. The ratios of these values between cases with and without mechanical stabilisation of the sub-ballast are presented in Figure 7. It can be seen that the ratio is dependent on the total ballast and sub-ballast thickness h. The higher track bearing capacity with mechanically stabilised sub-ballast would correspond with a lower mobilisation ratio compared with a non-stabilised section under the same wheel load. With permanent subgrade deformation predicted in terms of mobilised bearing capacity, as described by Lees and Kelly

(2023), this would translate into lower permanent subgrade deformation. In other words, thinner mechanically stabilised sub-ballast layers could be constructed to achieve the same performance in terms of subgrade deformation accumulation as thicker non-stabilised sub-ballast layers. This would bring economies in construction in terms of cost, time and carbon footprint.

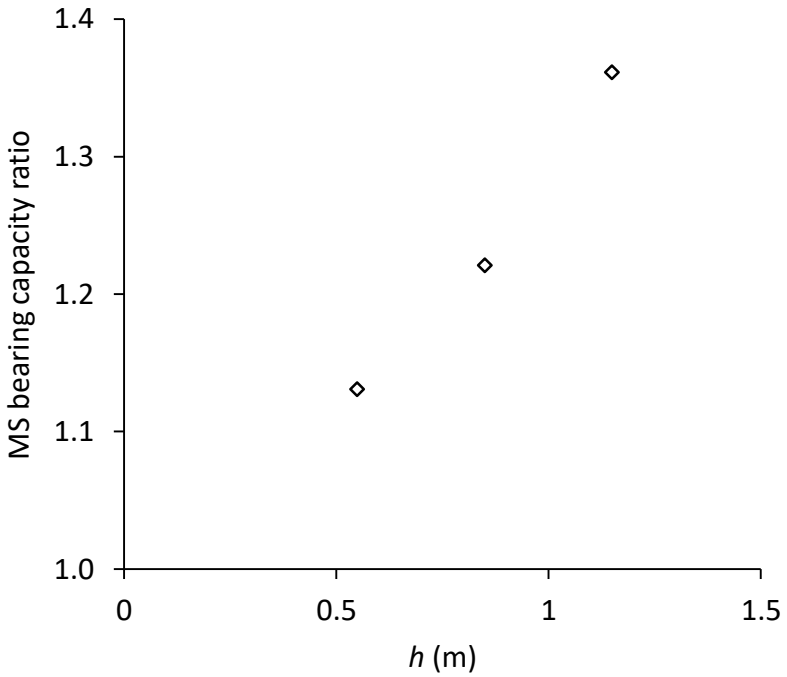

Fig. 7 Output of track bearing capacity ratio between mechanically stabilised and non-stabilised sub-ballast in all cases

FURTHER RESEARCH

Track formation designs with mechanically stabilised sub-ballast can be undertaken by FEA using the approach described by Lees and Kelly (2023) and adopting the TSSM for the sub-ballast layer as described by Lees and Clausen (2020). With more extensive parametric studies, relationships between mobilised subgrade strength and permanent strain and between mobilised track bearing capacity and permanent subgrade deformation could be established. This would streamline the design process significantly because the effect of variables such as wheel load and subgrade strength could be considered without the need for further FEM. Equations 1 and 2 could be used to predict the accumulation of subgrade strain and deformation following the Li and Selig (1998b) approach.

Historically, very little research is available where subgrade deformation has been measured at full scale. Studies such as these are required to validate advanced, performance-based design methods such as the one described in this paper. Furthermore, design methods incorporating the benefits of geosynthetics installed in the sub-ballast layer need physical validation test data. Those that include subgrade deformation measurement seem to be limited only to those by Hornicek (2022). Further useful insights would be gained from

physical studies into the geotechnical properties of subgrade soils and ballast layers that most affect the accumulation of permanent subgrade deformation.

CONCLUSIONS

A design method for railway track formations comprising ballast and sub-ballast or capping layers stabilised using stiff, coextruded, punched and drawn, multi-axial and multi-aperture shape geogrid to limit deformations in fine-grained subgrades has been proposed. It is based on previous performance-based design methods with the important distinction that advanced hardening plasticity constitutive models are used for the subgrade to predict permanent deformation under a single loading directly by FEM, rather than by elastic analysis and approximate empirical transfer functions. Permanent deformations from single loadings are then multiplied by simple, more reliable empirical relationships to include their accumulation from load repetitions during the design life of a railway track.

A small parametric study demonstrated the benefits of mechanical stabilisation of sub-ballast layers in terms of reduced subgrade stresses and increased track bearing capacity. These manifest themselves as decreased subgrade permanent strain and deformation. As such, equivalent performance as non-stabilised sub-ballast layers can be obtained with thinner mechanically stabilised sub-ballast layers. This would bring substantial economies in the construction and renewal of track formations.

It is recommended that continuous monitoring of subgrade characteristics (e.g. moisture content, suction) and subgrade deformation coupled with traffic tonnage be undertaken on reconstructed lines with mechanically stabilised sub-ballast on fine-grained subgrades. The paucity of such data seriously limits the extent of validation of new modelling and design approaches based on subgrade deformation that is possible. Yet, the potential cost savings of more economical formation designs far outweighs the cost of such investigations.

REFERENCES

Anon. (2021) Plaxis 3D Reference Manual. Bentley, 14 December.

Brinkgreve R.B.J., Zampich, L.M. and Ragi Manoj, N. (2019) *Plaxis Connect Edition V20*. Plaxis bv, Delft, The Netherlands.

Bussert F. and Cavanaugh J. (2010). Recent research and future implications of the actual behaviour of geogrids in reinforced soil. ASCE Earth Terention Conference (ER2010), 1-4 August, Bellevue, Washington, 460-477

Burrow, M.P.N., Shi, J., Wehbi, M. and Ghataora, G.S. (2017). Assessing the damaging effects of railway dynamic wheel loads on railway foundations, *Transportation Research Record* **2607**: 62-73.

Connolly, D.P., Dong, K., Alves Costa, P., Soares, P. and Woodward, P.K. (2020) High speed railway ground dynamics: a multi-model analysis, *International Journal of Rail Transportation* **8(4)**: 324-346.

D'Ignazio, M., Länsivaara, T.T. and Jostad, H.P. (2017). Failure in anisotropic sensitive clays: finite element study of Perniö failure test, *Canadian Geotechnical Journal* **54(7)**: 1013-1033.

Gräbe, P.J. and Clayton, C.R.I. (2009). Effects of principal stress rotation on permanent deformation in rail track foundations, *Journal of Geotechnical and Geoenvironmental Engineering* **135(4)**: 555-565.

Grimstad, G., Andresen, L. and Jostad, H.P (2012). NGI-ADP: Anisotropic shear strength model for clay, *International Journal for Numerical and Analytical Methods in Geomechanics* **36**: 483-497.

Karlsrud, K., Lunne, T., Kort, D.A. and Strandvik, S. (2005). CPTU correlations for clays, *Proceedings of the 16th International Conference on Soil Mechanics and Geotechnical Engineering, Osaka, Japan, 12-16th September*. IOS Press: Amsterdam.

Khan M.A. Strength-deformation behavior of a weathered clay crust, Ph.D. Thesis, Department of Civil Engineering, University of Ottawa, Canada; 1993.

Lees A., Kelly 2023. Railway formation design by elasto-plastic FEM mechanistic-empirical approach. Transportation Geotechnics, 39, 100955

Lees and Clausen, 2020 Lees AS, Clausen J. (2020). The strength envelope of granular soil stabilised by multi-axial geogrid in large triaxial tests. Can Geotech J 2020;57(3):448–52.

Li D, Hyslip J, Sussmann T and Chrismer S (2016) Railway Geotechnics CRC Press

Li, D. and Selig, E.T. (1998a). Method for railroad track foundation design I: Development, *Journal of Geotechnical and Geoenvironmental Engineering* **124(4)**: 316-322.

Li, D. and Selig, E.T. (1998b). Method for railroad track foundation design II: Applications, *Journal of Geotechnical and Geoenvironmental Engineering* **124(4)**: 323-329.

Sayeed, M.A. and Shahin, M.A. (2018a) Design of ballasted railway track foundations using numerical modelling. Part I: Development, *Canadian Geotechnical Journal* **55(3)**: 353-368.

Sayeed, M.A. and Shahin, M.A. (2018b) Design of ballasted railway track foundations using numerical modelling. Part II: Applications, *Canadian Geotechnical Journal* **55(3)**: 369-396.

Schanz, T., Vermeer, P.A. and Bonnier, P.G. (1999). The hardening soil model: formulation & verification. *Beyond 2000 Computational Geotechnics* (Brinkgreve, ed.). Balkema: Rotterdam, 281–290.